A comparison of warm and lower temperature processing routes for the equal-channel angular pressing of pure titanium

Asli G. Bulutsuz[*,1], Withold Chrominski[2], Yi Huang[3,4], Petr Kral[5], Mehmet Emin Yurci[1], Malgorzata Lewandowska[2], Terence G. Langdon[3]

[1]Yildiz Technical University, Department of Mechanical Engineering, 34349 Besiktas, Istanbul, Turkey
[2]Warsaw University of Technology, Faculty of Materials Science and Engineering, Woloska 141, 02-507 Warsaw, Poland
[3]Materials Research Group, Department of Mechanical Engineering, University of Southampton, Southampton SO17 1BJ, U.K.
[4]Department of Design and Engineering, Faculty of Science and Technology, Bournemouth University, Poole, Dorset BH12 5BB, U.K.
[5]Institute of Physics of Materials, ASCR, Zizkova 22, CZ -61662 Brno, Czech Republic

Highlights

- A new combined temperature processing route was used for ECAP
- The novel route was successful to improve strain rate in the microstructure
- Conventional ECAP processing route had more homogenous hardness distribution
- Different process temperature effects on microstructure during ECAP are discussed

Abstract

In this study, equal-channel angular pressing (ECAP) applied to pure titanium samples with different temperatures for successive pressing. The aim here is increasing process efficiency without applying any further heat treatment or thermomechanical process. In order to understand the effects of this new route with different temperature on the structure, TEM, EBSD measurements were applied. For understanding temperature effect on the mechanical properties tensile tests and micro hardness tests were applied. Moreover for assessment of the microstructural homogeneity color coded maps for hardness were obtained. The microstructural results showed the strain rate of the pressing temperature combined specimen were higher than warm pressed sample. However the color coded hardness map indicated in non-homogeneous hardness for pressing temperature combined specimen vis-à-vis 2 passes at 450 °C pass specimen. Application of combined temperature increased strength besides the final grain size was smaller than 2 times pressed at 450 °C sample.

*Corresponding author: asligunay@gmail.com, +90 2123532959

1. Introduction

Equal-channel angular pressing (ECAP) is an effective processing tool for strengthening a wide range of metals including titanium through the introduction of significant grain refinement [1]. This severe plastic deformation technique is a well-established method to increase materials mechanical properties without the necessity of alloying [1-3]. Generally for titanium, Al and V are chosen as alloying elements which are allergic and toxic to body [4-6]. Pure titanium (Grade 4) is a popular material and being used by various manufacturing areas such as aerospace, military, biomedical applications due to its superior corrosive, mechanical behaviors and good biological compatibility to the body [7]. Besides these properties pure titanium has a lower c/a ratio, 1.58 than ideal. As it is known according to the von Mises and Taylor criteria for an arbitrary strain accommodation five independent slip system have to be active as given in Eq. 1 because pure glide cannot change the crystal density as given in Eq. 2;

$$\varepsilon_{ij}^{(T)} = \sum_k \varepsilon_{ij}^{(k)} \tag{1}$$

$$\varepsilon_{11}^{(T)} + \varepsilon_{22}^{(T)} + \varepsilon_{33}^{(T)} = 0 \tag{2}$$

As given in [8] HCP structured pure titanium (Grade 4) for $< 11\bar{1}0 >$ slip there are maximum four independent slip system. Thus, pure Ti is not a candidate for homogenous plastic deformation with its dependent slip systems. However, material exhibits a good ductility with its additional twinning systems that accompanies to slip systems [8-11]. Microstructural and crystal structure changes in materials after the ECAP which is obtained with slip of dislocations and the formation of boundaries. Due to above mentioned reasons and pure titanium low stacking fault energy and hexagonal-close-packed crystallography the deformation behavior during ECAP processing is different from face-centered-cubic (FCC)

and body-centered-cubic (BCC) materials. Among this crystallography during slip HCP requires deformation twinning besides of slip of grains, for deformation twins are more common in the microstructure [12]. Higher process temperature enable deformation of hexagonal close packed (hcp) structure pure titanium with activation of additional slip system - deformation twinning [13-15]. The formation of twins during the pressing is mainly affected by processing temperature. For example at ambient temperature there are three different twinning planes $\{10\bar{1}2\}$, $\{11\bar{2}1\}$ and $\{11\bar{2}2\}$, for 350 ˚C a new $\{10\bar{1}1\}$ twining plane is activated [15-17]. Thus, the amount of twinning and slip systems in the microstructure of the material is depend on the process temperature and strain rate. Different deformation mechanism results in various final microstructure and mechanical properties including ductility [16, 18].

In order to apply a successful severe plastic deformation there are some important properties such as; submicron grain size, higher strength, good surface finish and homogenous microstructure. Detailed experimental studies investigated different SPD processes in order to provide these properties for a successful procedure. Besides, homogenous microstructures were being investigated by researchers for different SPD methods and their parameters [19-22]. Hardness measurements are a strong tool to understand microstructural strain homogeneity. Some of the studies focused on the effect of deformation method on homogeneity [19, 20], some of them focused on the effect of process parameters [21-23, 25]. In [23], HPT procedure was used and the numbers of turn were investigated and after 5 turns the hardness distributions were found to be homogenous. The non-homogenous microstructure forms due to the strain variations along the disk diameter of the sample. From this point of view ECAP is more successful because strain distribution in the deformation area for each pass is more homogenous than that in HPT sample along the diameter of the disk. The microstructure can be in-homogenous due to the friction of sample surface, dead area and

stress flow that changes with process parameters such as extrusion velocity or process temperature. In [21], effect of strains on micro structures homogeneity were investigated in detail and four passes found to be enough for a homogenous microstructure. In [22], outer round corner of die effect were investigated on the flow homogeneity in ECAP procedure and no measurable differences were observed. In [2, researchers investigated ECAP slip systems and their effect on the microstructure and for elevated temperatures mostly. In their search it was obtained that pyramidal slip systems were active. As a results the non-homogenous microstructure were observed.

Besides effect of process temperature on the microstructure, manufacturing at higher temperature increases the risk of undesired grain growth in microstructure [24]. Also, working at lower temperatures is more convenient for mass production. Nevertheless working at ambient temperature has risks such as segmentation due to titanium poor shear plane and short extrusion mold life due to high friction between titanium and mold. Thus, generally titanium is pressed at warmer temperature which is equal or lower than 450 ˚C.

Since pure titanium of grade 4 represents an optimum material for medical implants based on toxicity considerations, and because processing by ECAP is a simple and reproducible processing technique, the present investigation was initiated to determine the potential for opimizing the microstructure, homogeneity and mechanical properties of this material. Two different processing routes were evaluated: a so-called combined temperature route (CT) is which the temperature was changed between the first and second pass of ECAP and a so-called warm temperature route (WT) where the temperature was maintained at a high level for two co9nsecutive passes. The microstructures and mechanical properties were then evaluated using TEM and EBSD methods combined with tensile testing and microhardness measurements.

2. Experimental material and procedures

The experimental material was commercial purity titanium (CP-Ti) of grade 4 which was annealed at 700°C for 4 hours to give an initial average grain size of ~58 μm. Billets for ECAP processing were cut as cylinders with lengths of 20 mm and diameters of 5 mm. These billets were processed using an ECAP die having an internal channel angle, Φ, of 110° and an outer arc of curvature, Ψ, close to 0°. These angles produce a strain of ~0.81 on each separate pass through the die. After pressing for one pass the billet was rotated about the longitudinal axis by 90˚ in route B_c [10]. Two sets of specimens were used in these experiments. First, billets were pressed in the group was initial state. The other two specimens were pressed for up to 2 passes using a ram speed of 0.1 mm/s with two different temperature schemes as shown in Table 1. In combined temperature (CT) scheme, the specimen was firstly pressed at 450 ˚C afterwards pressed at 100 ˚C. In warm temperature (WT) scheme, the specimen was pressed 2 times at 450 ˚C. A lubricant containing MoS_2 was used for both of samples and ECAP die.

The microstructures of specimens were examined with an optical microscope and with a scanning electron microscope (SEM) on both polished and etched surfaces. For EBSD observations, a Tescan Lyra 3 SEM equipped with a NordlysNano EBSD detector was used with an accelerating voltage of 20 kV. The EBSD data were subsequently analyzed using HKL Channel 5 software (Oxford Instruments). In order to determine the misorientations between grains, grain angles above 15° were designated high-angle grain boundaries (HAGBs) and angles below 15° were designated low-angle grain boundaries (LAGBs). For transmission electron microscopy (TEM), standard 3 mm disks were cut from the ECAP processed billets and thin regions were prepared using double-jet polishing in a methanol-perchloric acid bath (ratio of 4:1). The TEM observation were conducted in a JEOL JEM 1200 EX II microscope operating at 120 kV.

Dog-bone shape tensile specimens were cut from the central regions of the pressed billets with gauge lengths of 15.0 mm parallel to the pressing axes and gauge widths and thicknesses of 4.0 and 1.5 mm, respectively. Specimens were cut by wire erosion and the surfaces were ground to remove any effects from the machining operation. A special tensile test apparatus was fabricated to accommodate these small specimens in the tensile machine. Tensile tests were performed at room temperature under conditions of constant crosshead displacement using an initial strain rate of $1.0 \times 10^{-3}\ s^{-1}$ and the stress-strain curves were then examined to determine the yield strength, σ_{ys}, the ultimate tensile strength, σ_{UTS}, and the elongation to failure, δ%.

A Vickers microhardness tester (HVS1000) was used to obtain hardness maps over the cross-sections of billets on surfaces cut perpendicular to the pressing direction. Measurements were taken at 85 different points on each surface using an array of 0.4 mm steps as depicted schematically in Fig. 1 with each measurement taken using a load of 200 g for a dwell time of 10 s. These measurements were used to construct color-coded maps providing a visual display of the microhardness values.

3. Experimental results

3.1 Microhardness measurements and tensile testing

The measured values of the mean microhardness for samples processed under these two processing conditions are Hv ≈ 272 for CT and Hv ≈ 245 for WT where these val;ues correspond to hardnesses of ~2650 and ~2350 MPa. By comparison, there was a measured microhardness of Hv ≈ 180 (~1760 MPa) for the initial annealed material without ECAP processing. Thus, processing by ECAP produces a significant increase in strength and hardness after only a single pass as noted also in experiments conducted on a number of commercial aluminum-based alloys [11 horita MMT].

The homogeneity of the hardness measurements across the cross-sectional planes on the ECAP billets is shown by the color-coded maps presented in Fig. 2 for processing under (a) CT and (b) WT conditions, where the data are plotted such that the *X* and *Y* scales are perpendicular orientations positioned arbitrarily such that the points (0,0) are located at the centers of the cross-sections of the two billets; the absolute values of the hardness values are indicated by the keys on the right of each diagram. Thus, the hardness values are consistently higher for CT than WT and this is reasonable because of the potential for grain growth when pressing at higher temperatures. Nevertheless, there is a reasonable hardness homogeneity for both processing conditions throughout the cross-sections and there is no clear evidence for regions of lower hardness, having thicknesses of ~0.5 mm, lying adjacent to the lower surfaces of the billets as reported earlier after processing an Al-6061 alloy by up to 6 passes of ECAP at room temperature [12 Prell 2008-449].

In order to determine the strength of specimens, tensile testing was conducted at room temperature using an initial strain rate of 1×10^{-3} s^{-1}. From these tests, the values of the yield stress and maximum tensile strength were recorded and the results are shown in Table 1 where the upper row corresponds to the initial annealed condition without ECAP processing. Thus, and consistent with the microhardess data, there is an increase in strength after ECAP processing and this increase is larger when processing under CT conditions.

3.2 Microstructural evolution

Representative microstructures are shown in Fig. 3 for samples processed under (a) CT and (b) WT conditions. For both images, there are inhomogeneous microstructures formed by a mixture of ultrafine-grained areas containing predominantly HAGBs and some exceptionally large grain areas containing predominantly LAGBs. According to the statistical data, Fig. 3(a) contains a higher ratio of HAGBs than Fig. 3(b). Moreover, based on TEM observations, the

microstructure in Fig. 3(b) for the WT condition contains more subgrains and the ultrafine grain sizes tend to be relatively smaller than for the CT condition.

The grain size distributions are shown in Fig. 4 for samples processed for 2 passes by (a) the CT and (b) the WT conditions. For the CT condition, the ultrafine grains occupy up to ~20 % of the total area and this is larger than for the WT condition. Nevertheless, several grains exceeding 10 μm were found in the CT microstructure and these large grains occupied ~30 % of the investigated area in the CT sample. The mean grain size in the CT sample was ~1.5 μm with about 40% of HAGBs and no grains larger than ~17 μm whereas the mean grain size in the WT condition was ~1.7 μm with a slightly higher fraction of ~45% of HAGBs. It is apparent from Fig. 4 that the WT sample has a slightly wider grain size distribution than the CT sample.

Figure 5 shows the inverse pole figures in (a) the CT sample and (b) the WT sample where (c) defines the coordinate system in the ECAP billet. In the CT sample in Fig. 5(a), the basal poles of grains are tilted about 20-45° away from the *Y* axis, the majority of grains have a tendency to orient to $\{10\bar{1}2\}$ planes parallel with the pressing direction of the last pass, where this corresponds to the longitudinal plane *XZ* parallel to the channel side wall. The $< 11\bar{2}0 >$ directions are oriented nearly parallel with the pressing direction which corresponds to the *X* axis. Thus, this microstructure for the CT sample has a relatively strong $\{10\bar{1}2\} < 11\bar{2}0 >$ microtexture. In the WT sample, Fig. 5(b) shows the predominant tendency is to orient in the $< 11\bar{2}0 >$ directions parallel to the pressing direction and with the majority of grains there is a tendency to form basal poles parallel with the *Y* axis, where this means with {0001} planes parallel with the pressing direction of the last pass corresponding again to the longitudinal plane *XZ* parallel to the channel side wall. Nevertheless, the texture of the WT sample appears to be more random than the CT sample and in the WT sample the microstructure has relatively strong $\{0001\} < 11\bar{2}0 >$ and weak $\{10\bar{1}0\} < 11\bar{2}0 >$ microtextures.

In the initial unprocessed condition the average grain size was ~58 μm and there was evidence for some precipitate particles within the grains. Figure 6(a) shows a low magnification TEM image of material processed by ECAP under CT conditions and a higher magnification image is shown in Fig. 6(b). The non-uniform levels of shading in these images suggest the presence of high internal stresses which are a direct consequence of the SPD processing, where this is consistent with the detailed synchrotron X-ray microbeam diffraction measurements reported earlier for samples of an Al-1050 alloy processed by multiple passes of ECAP at room temperature [Phan AM 2016]. Thus, there are almost no sharp changes in the strain contours which is a direct consequence of the residual stresses. From these observations itr is reasonable to conclude that there is only a single grain in the field of view in Fig. 6(a). In the higher magnification image in Fig. 8(b) there is a high density of dislocations within the observed area and these dislocations are relatively homogenously distributed. Again the strain contours show non-uniform diffraction conditions in relatively small areas. It should be noted also that the dark contours are continuous so that there are no dislocation walls or LAGBs within this image.

Similar sets of lower and higher magnification images are shown in Fig. 7(a) and (b) for the WT conditions. In the lower magnification image in Fig. 9(a) there are features that were not apparent in the CT images in Fig. 6. Thus, the level of shading is again non-uniform over the whole image but there are sharp changes, marked with arrows, which denote the presence of LAGBs. In the higher magnification image in Fig. 9(b) there are sub-grains filled with reasonably homogenously distributed dislocations and the neighboring grains vary in their contrast within the matrix which suggests slight differences in their orientations.

4. Discussion

As observed from TEM results both 2 pass samples include high strain inside of grains. Despite of same number of ECAE and high strain inside microstructure, their mechanical

strength differs. Moreover from EBSD images it is observed that CT sample has wider grain size distribution than WT sample. As can be seen from TEM image (Fig. 8a), inside the CT specimen grains, high density of dislocations relatively homogenously distributed within the observed area. Moreover, there were no dislocation walls within grains and contours were continuous that signs the angles between grains were high. As can be seen from tensile test results (Table 2) the CT sample has relatively higher strength. The angle between grains considered to be reason of these results. As shown in Fig. 9a WT sample had more grain boundary under same magnification with CT specimen. Moreover in this figure there are slight, direct borders between grains which declares lower boundary angle.

According to the applied mechanical test and optical observations on ECAP processed samples with different temperature scheme, differently mechanical properties were observed between CT and WT samples. Significant differences were observed for hardness homogeneity and tensile strength especially. In a previous experimental study the authors obtained more homogenous microstructure with 8 times pressed specimen than both of these 2 times pressed samples. Which reveals the strain was not enough to manufacture homogenous micro structure [21]. The differences between two times pressed samples was attributed to their various deformation mechanisms due to the different process temperature. As highlighted in [27], pure titanium generally deforms with slip at 200 °C process temperatures. Above 250 °C the specimen accommodates the strain with twinning in the microstructure. From this point of view deforming at 100 °C degree, higher strain can be accommodated with less stress due to the grain boundary sliding [27,28].

5. Summary and conclusions

In this work, ECAP processing with combined temperature scheme and warm temperature scheme was successful conducted for manufacturing of highly deformed CP-Ti. Application

of combined temperature was proved to be slightly more efficient than regular route for improving tensile strength and the following conclusions can be made:

- The combination of low temperatures with warm temperatures significantly affects specimen microstructures after processing two passes.
- EBSD measurements indicated that CT specimen showed smaller HAGBs (%40) and smaller mean grain size 1.55 μm. higher process temperature for two passes ACEP result with higher HAGBs (%45) with bigger grain size 1.71 μm
- The differences of mechanical and microstructural properties can be attributed to the different slip systems, grain growth and recrystallization due to the process temperatures. Moreover it is known process temperature is a strong tool that effect strain distribution and dislocation mobility during the deformation.
- Mechanical results indicate combined temperature increased mechanical strength and hardness besides decreased homogeneity in grain size distributions.

Generally to improve effectiveness of severe plastic deformation, cold deformation methods applied afterwards SPD process. Differently, in this experimental study lower temperature were used for subsequent ECAP passes in order to observe its effect on micro structure and mechanical properties. As a future study different combination of low and high temperatures routes for higher pass numbers is planned to apply in order to understand its effect at higher dislocation densities.

Acknowledgements

The authors thank the Technical Electrical Materials Industry and Trade Inc. for their technical support. Two of the authors (YH and TGL) were supported by the European Research Council under ERC Grant Agreement no. 267464-SPDMETALS.

References

[1] L. Wang, Y. Yang, P. Eisenlohr, T.R. Bieler, M.A. Crimp, and D.E. Mason, Twin nucleation by slip transfer across grain boundaries in commercial purity titanium, Mason: Metall. Mater. Trans. A Phys. Metall. Mater. Sci., 41(2010) , 421–30.

[2] D.H. Shin, B.C. Kim, K.T. Park, and W.Y. Choo, Microstructural changes in equal channel angular pressed low carbon steel by static annealing Acta Mater.,48(2000), 3245–52.

[3] Y. Iwahashi, M. Furukawa, Z. Horita, M. Nemoto, and T.G. Langdon, Microstructural characteristics of ultrafine-grained aluminum produced using equal-channel angular pressing Metall. Mater. Trans. A, 29 (1998) , 2245–52.

[4] D.H. Shin, I. Kim, J. Kim, Y.S. Kim, and S.L. Semiatin, Microstructure development during equal-channel angular pressing of titanium, Acta Mater., 51 (2003), 983–96.

[5] A. Jäger, V. Gärtnerova, and K. Tesař, Microstructure and anisotropy of the mechanical properties in commercially pure titanium after equal channel angular pressing with back pressure at room temperature, Mater. Sci. Eng. A, 644(2015), 114–20.

[6] H. Numakura, M. Koiwa, Hydride Precipitation In Titanium, Pers. in Hyd. in Met. (1986), 501-509

[7] I. Kim, W.-S. Jeong, J. Kim, K.-T. Park, and D.H. Shin, Deformation structures of pure Ti produced by equal channel angular pressing, Scr. Mater., 45 (2001), 575–80.

[8] M.H. Yoo, Slip, twinning, and fracture in hexagonal close-packed metals, Metall. Trans. A, 12A(1981), 409-18.

[9] M.H. Yoo, J.R. Morris, K.M. Ho, and S.R. Agnew, Nonbasal deformation modes of HCP metals and alloys: Role of dislocation source and mobility, Metall. Mater. Trans. A Phys. Metall. Mater. Sci., 33(2002), 813–22.

[10] G. Lütjering, J.C. Williams, Titanium, 2nd edition, Springer, pp.442.

[11] P. M. Anderson, John P. Hirth, Jens Lothe , Theory of Dislocations, 2nd Edition, pp.857.

[12] A.A. Salem, S.R. Kalidindi, and R.D. Doherty, Strain hardening of titanium: role of deformation twinning, Acta Mater., 51(2003), 4225–37.

[13] P.G. Partridge, The crystallography and deformation modes of hexagonal close-packed metals, Metall. Rev, 12(1967), 169–94.

[14] J.W. Christian, S. Mahajan, Deformation twinning Prog. in Mater. Sci., 39 (1995), 1–158.

[15] U.F. Kocks H. Mecking D.G Morris Igor V Alexandrov Terry C Lowe E. Ma R. Z. Valiev, Physics and phenomenology of strain hardening: the FCC case, Prog. in Mater. Sci.,48(2003), 171-273

[16] V. V. Stolyarov, Y.T. Zhu, T.C. Lowe, and R.Z. Valiev, Microstructure and properties of pure Ti processed by ECAP and cold extrusion, Mater. Sci. Eng. A, 303(2001), 82–9.

[17] R.Z. Valiev and T.G. Langdon, Principles of equal-channel angular pressing as a processing tool for grain refinement, Prog. Mater. Sci., 51(2006), 881–981.

[18] K. Sharman, P. Bazarnik, T. Brynk, A. G. Bulutsuz, M. Lewandowska, Y. Huang, and T.G. Langdon, Enhancement in mechanical properties of a β-titanium alloy by high-pressure torsion, J. Mater. Res. Technol., 2015, vol. 4, pp. 79–83.

[19] K.S. Suresh, M. Geetha, C. Richard, J. Landoulsi, H. Ramasawmy, S. Suwas, and R. Asokamani, Effect of equal channel angular extrusion on wear and corrosion behavior of the orthopedic Ti–13Nb–13Zr alloy in simulated body fluid, Mater. Sci. Eng. C, 32(2012), 763–

[20] I. Kim, J. Kim, D.H. Shin, C.S. Lee, and S.K. Hwang, Effects of equal channel angular pressing temperature on deformation structures of pure Ti, Mater. Sci. Eng. A, 342(2003), 302–10.

[21] W.J. Kim and H.T. Jeong, Grain-Size Strengthening in Equal-Channel-Angular-Pressing Processed AZ31 Mg Alloys with a Constant Texture, Mater. Trans., 46(2005), 251–8.

[22] R.Z. Valiev, A. V. Sergueeva, and A.K. Mukherjee, The effect of annealing on tensile deformation behavior of nanostructured SPD titanium, Scr. Mater., 2003, vol. 49, pp. 669–74.

[23] C. Xu, Z. Horita, and T.G. Langdon, The Evolution of Homogeneity in an Aluminum Alloy Processed Using High-Pressure Torsion, Acta Mater., 55(2007), 203–12.

[24] I. Mazurina, T. Sakai, H. Miura, O. Sitdikov and R. Kaibyshev, Partial Grain Refinement in Al-3%Cu Alloy during ECAP at Elevated Temperatures, Materials Transactions, Vol. 50, No. 1 (2009), 101 to 110.

[25] C. Xu and T.G. Langdon, Influence of a round corner die on flow homogeneity in ECA pressing, Scr. Mater., 48(2003), 1–4.

[26] A. Zhilyaev, N. Parkhimovich, G. Raab, V. Popov, and V. Danilenko, Microstructure And Texture Homogeneity Of Ecap Titanium, Rev. Adv. Mater. Sci., 43(2015), 61–6.

[27] A.P. Zhilyaev, G. V. Nurislamova, B.K. Kim, M.D. Bar, J.A. Szpunar, and T.G. Langdon, Experimental parameters influencing grain refinement and microstructural evolution during high-pressure torsion, Acta Mater., 51(2003), 753–65.

[28] M. Liu, B. Shi, J. Guo, X. Cai, and H. Song, Lattice constant dependence of elastic modulus for ultrafine grained mild steel, Scr. Mater., 49(2003), 167–71.

[29] K. Topolski, H. Garbacz, P. Wiecinski, W. Pachla, and K.J. Kurzydłowski, Mechanical properties of titanium processed by hydrostatic extrusion, Arch. Metall. Mater., 57(2012), 2–6.

[30] M. Nakai, M. Niinomi, J. Hieda, H. Yilmazer, and Y. Todaka, Heterogeneous grain refinement of biomedical Ti–29Nb–13Ta–4.6 Zr alloy through high-pressure torsion Sci. Iran., 20(2013), 1067–70.

[31] H. Yilmazer, M. Niinomi, M. Nakai, J. Hieda, T. Akahori, and Y. Todaka, Microstructure and mechanical properties of a biomedical β-type titanium alloy subjected to severe plastic deformation after aging treatment, Key Eng. Mater., 508 (2012), 152–60.

[32] R.Z. Valiev, E.V. Kozlov, Yu.F. Ivanov, J. Lian, A.A. Nazarov, B. Baudelet, Deformation behaviour of ultra-fine-grained copper, Acta Metal. Mater., 42 (1994), 2467–2475

[33] H.S. Kim and M.B. Bush, The effects of grain size and porosity on the elastic modulus of nanocrystalline materials, Nanostructured Mater., 11(1999), 361–7.

[34] K. Ozaltin, W. Chrominski, M. Kulczyk, A. Panigrahi, J. Horky, M. Zehetbauer, and M. Lewandowska, Enhancement of mechanical properties of biocompatible Ti–45Nb alloy by hydrostatic extrusion, J. Mater. Sci., 49(2014), 6930–6.

[35] T. D. Shen, C. C. Koch, T. Y. Tsui, and G. M. Pharr, On the elastic moduli of nanocrystalline Fe, Cu, Ni, and Cu–Ni alloys prepared by mechanical milling/alloying, J. Mater. Res.,10(1995), 2892.

[36] D. MA, O.C. Wo, J. Liu, and J. HE, Determination of Young's modulus by nanoindentation, Sci. China Ser. E, 2004, vol. 47, pp. 398

[37] H Matsumoto, S. Watanabe, S Hanada, Microstructures and mechanical properties of metastable b TiNbSn alloys cold rolled and heat treated, J Alloys Compd, (2007), 439, pp. 146–155

(a)

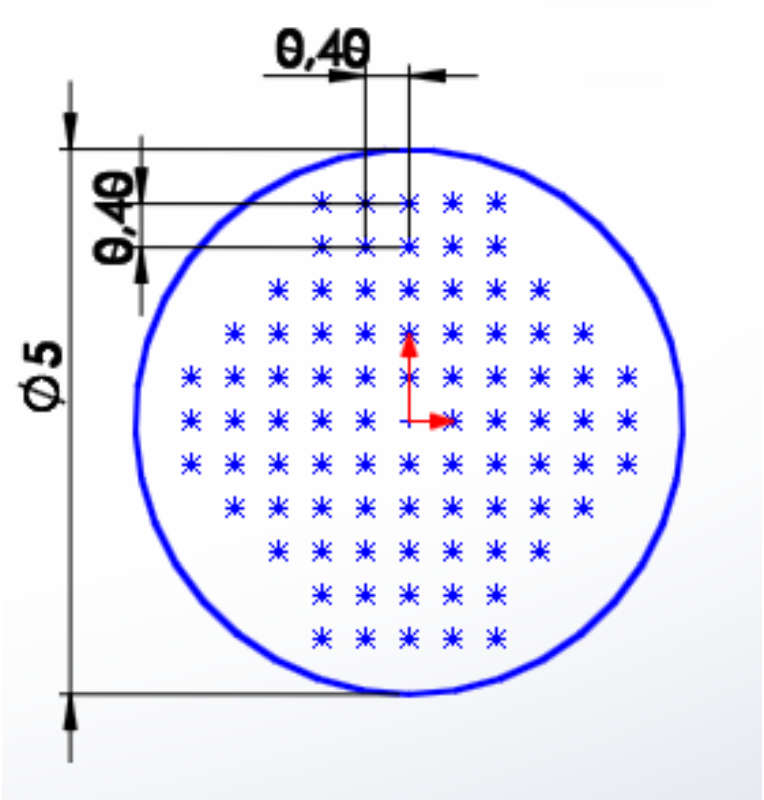

(b)

Fig. 1 (a) Microstructure of the initial CP-Ti; (b) Schematic show of measurement points for hardness mapping.

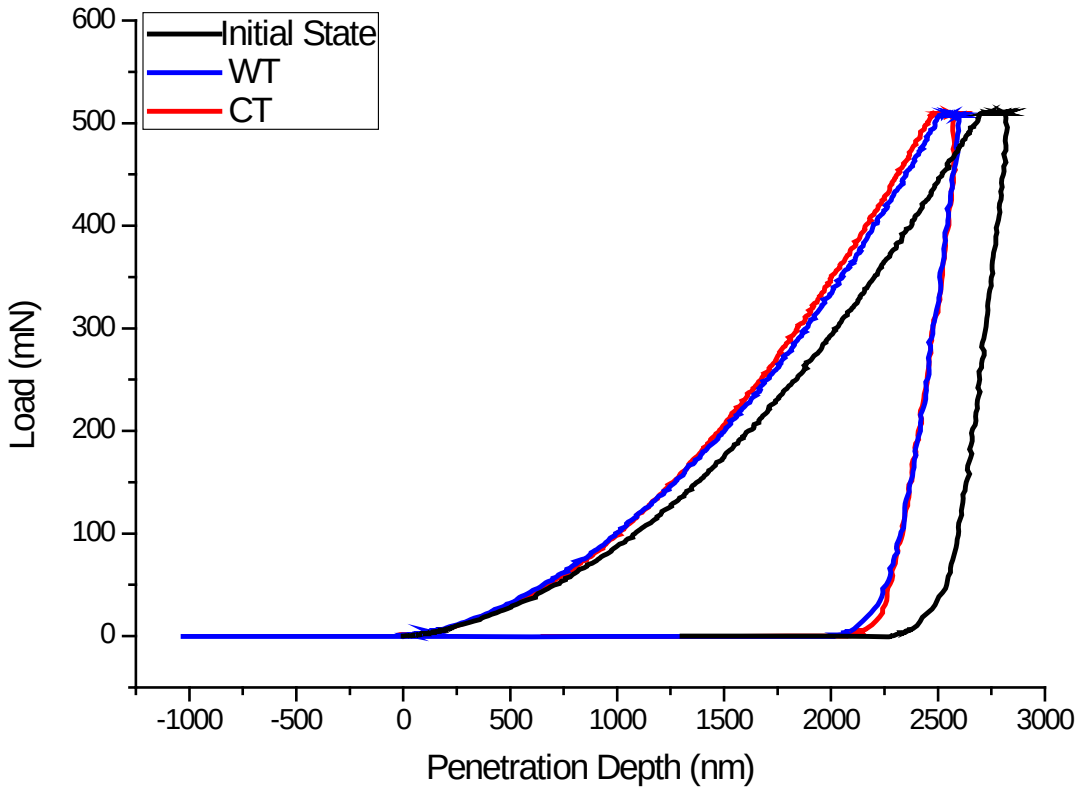

Fig. 2 Load-displacement curves for initial CP-Ti, and ECAP processed samples under CT and WT conditions

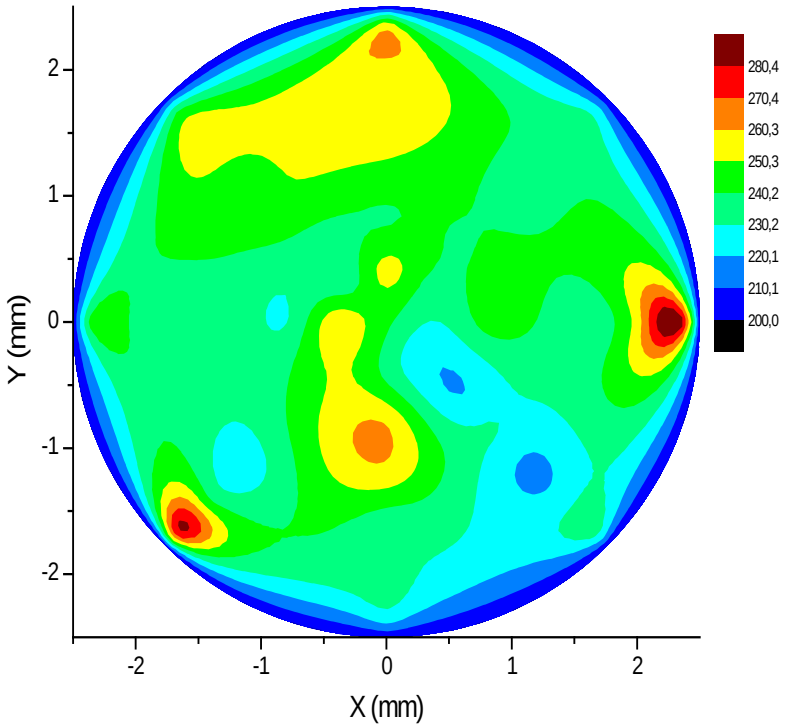

(a)

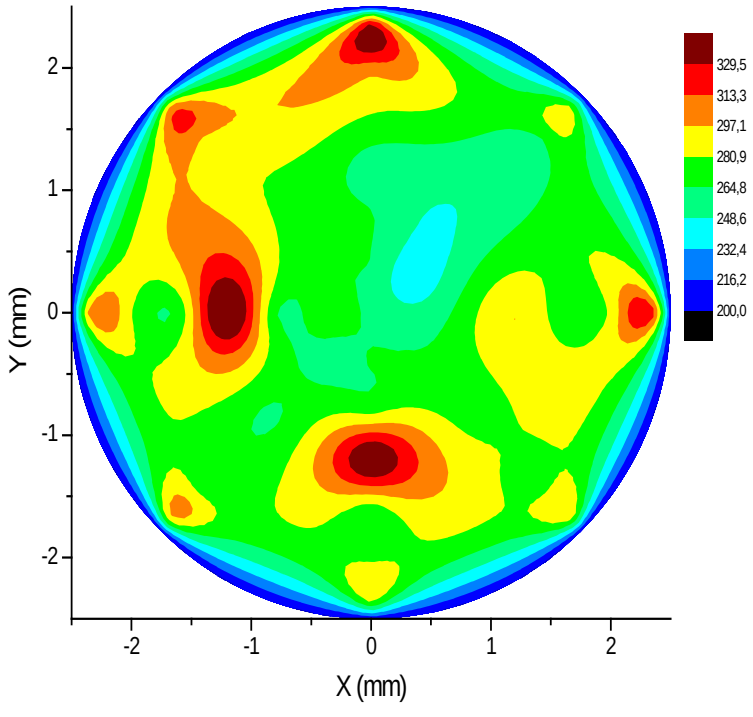

(b)

Fig. 3 Hardness mapping in ECAP processed samples under (a) WT and (b) CT conditions.

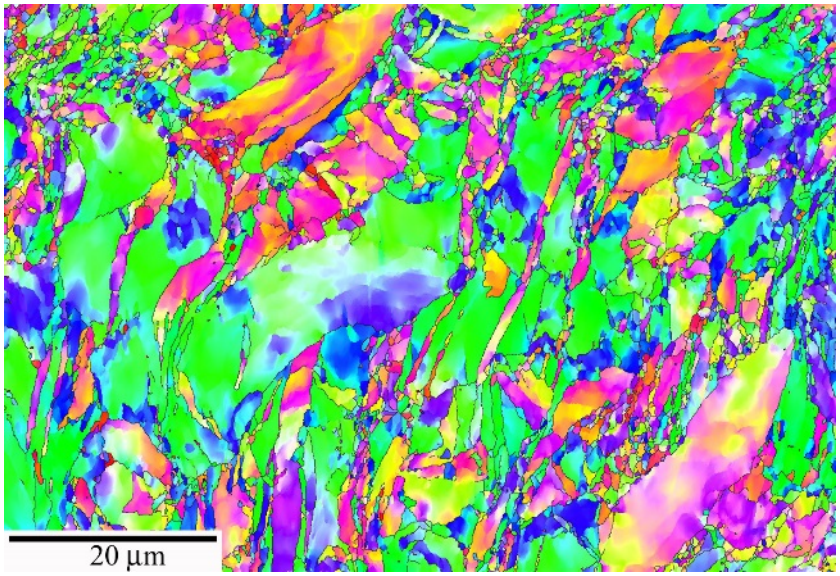

(a)

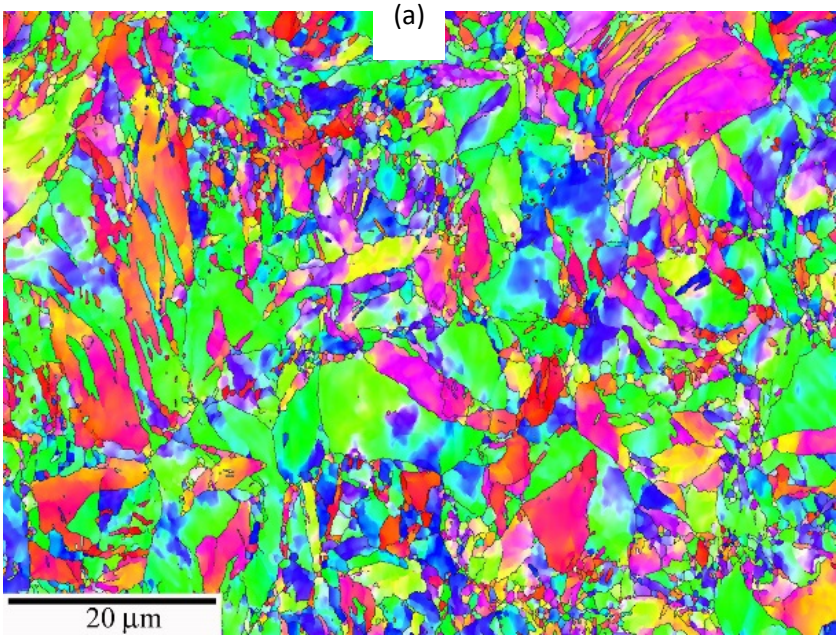

(b)

Fig. 4 The EBSD orientation maps of samples processed by ECAP under (a) CT and (b) WT conditions

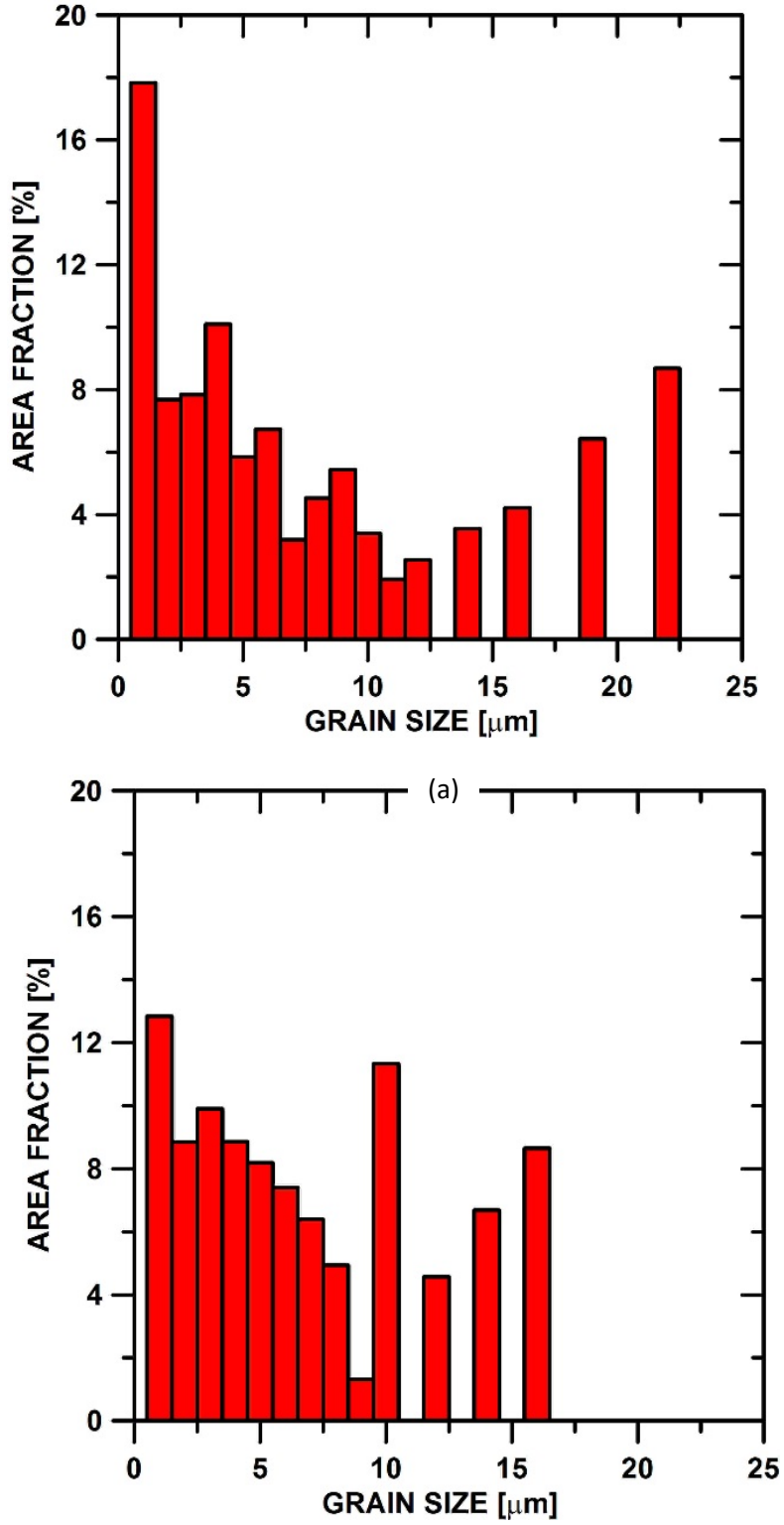

Fig. 5 Grain size distribution in samples processed ⊐AP under (a) CT and (b) WT conditions

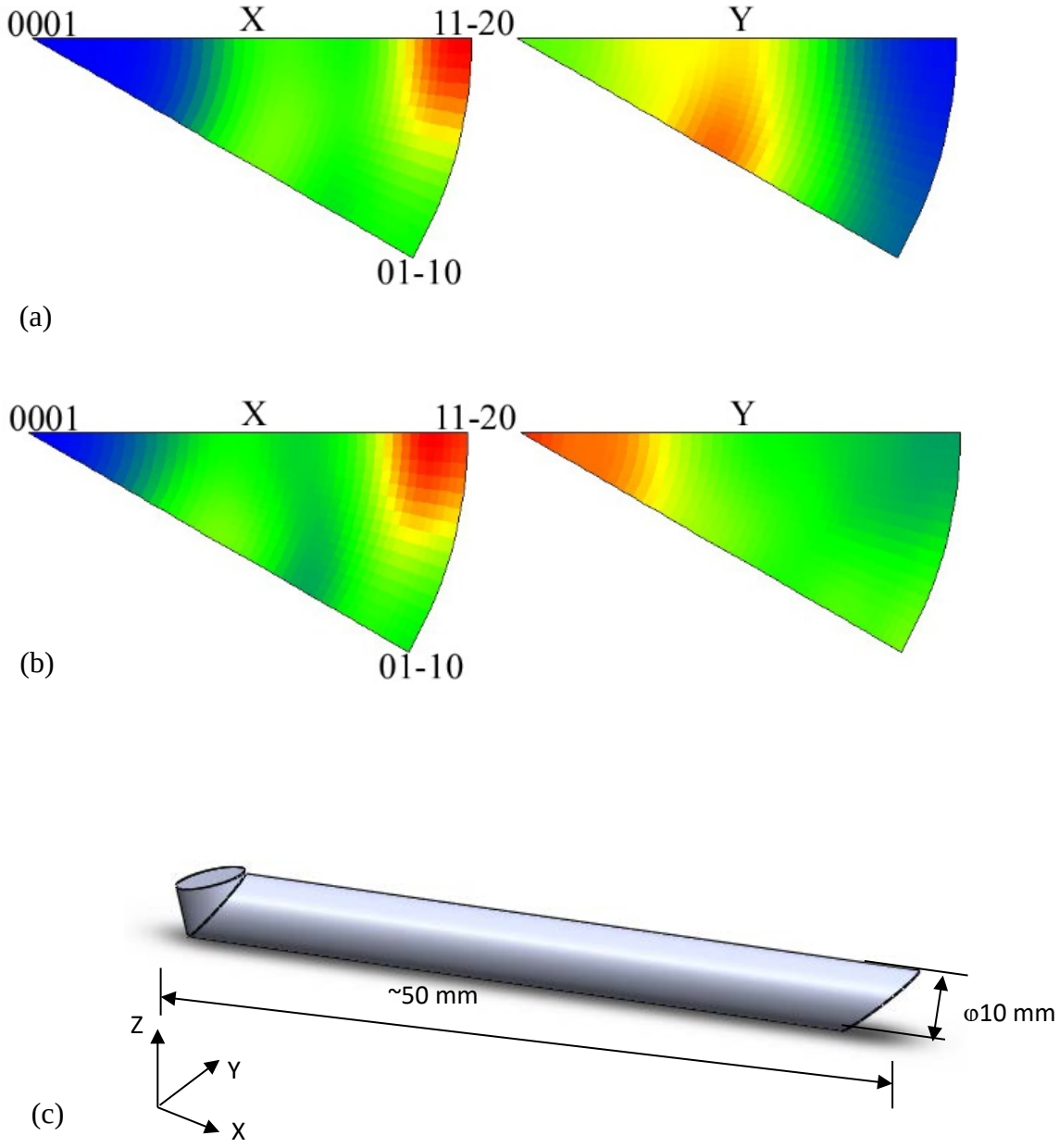

Fig. 6 Inverse pole figures obtained for the pressing direction (axis X) and longitudinal section (axis Y) in (a) CT sample and (b) WT sample (c) ECAP Processing axis.

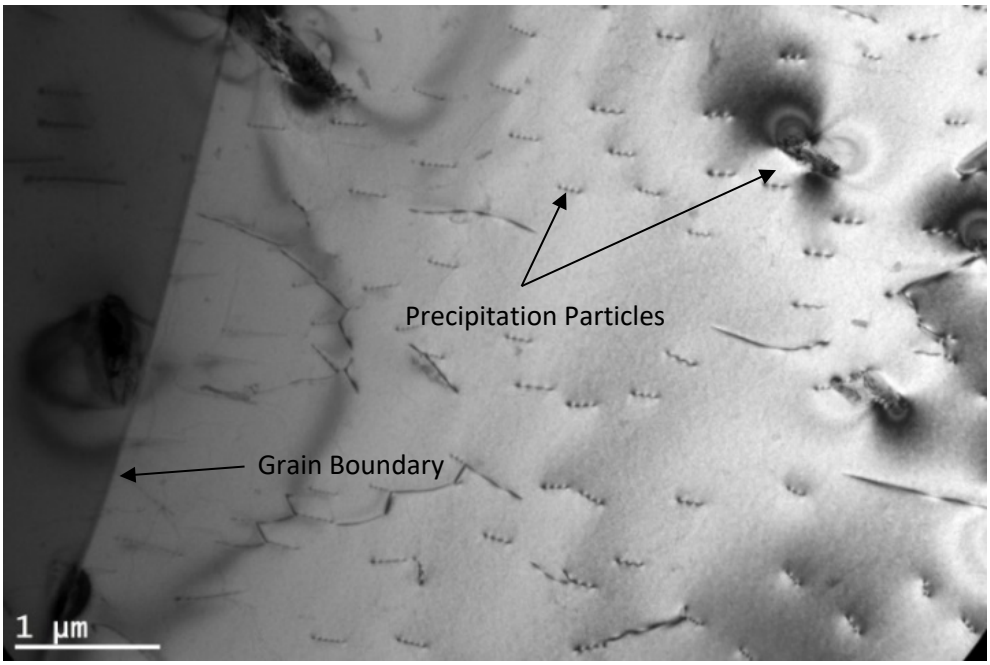

Fig. 7 TEM image of CP-Ti in initial condition

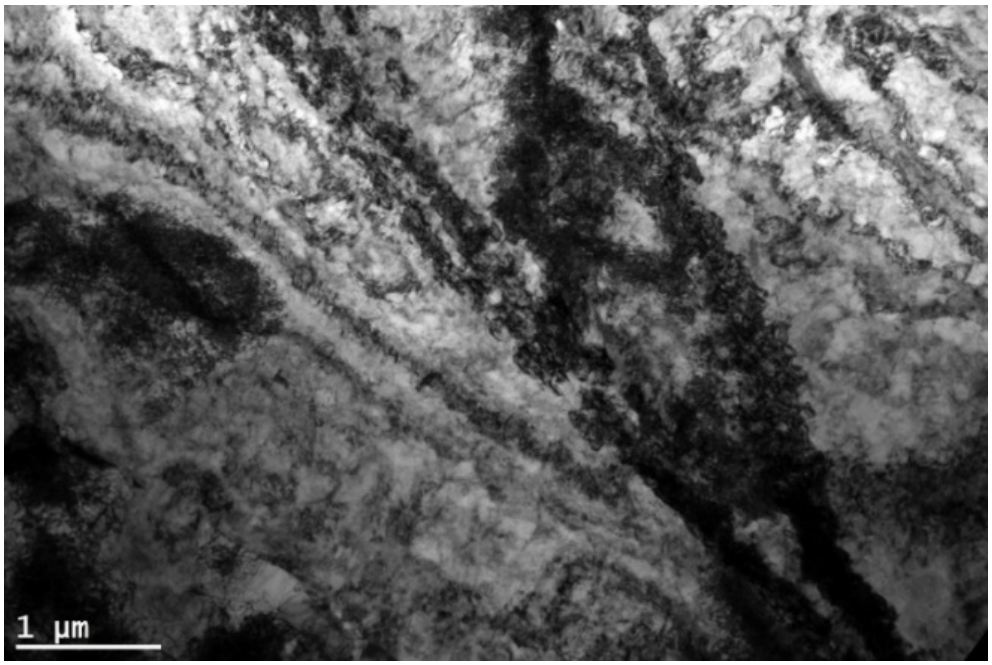

(a)

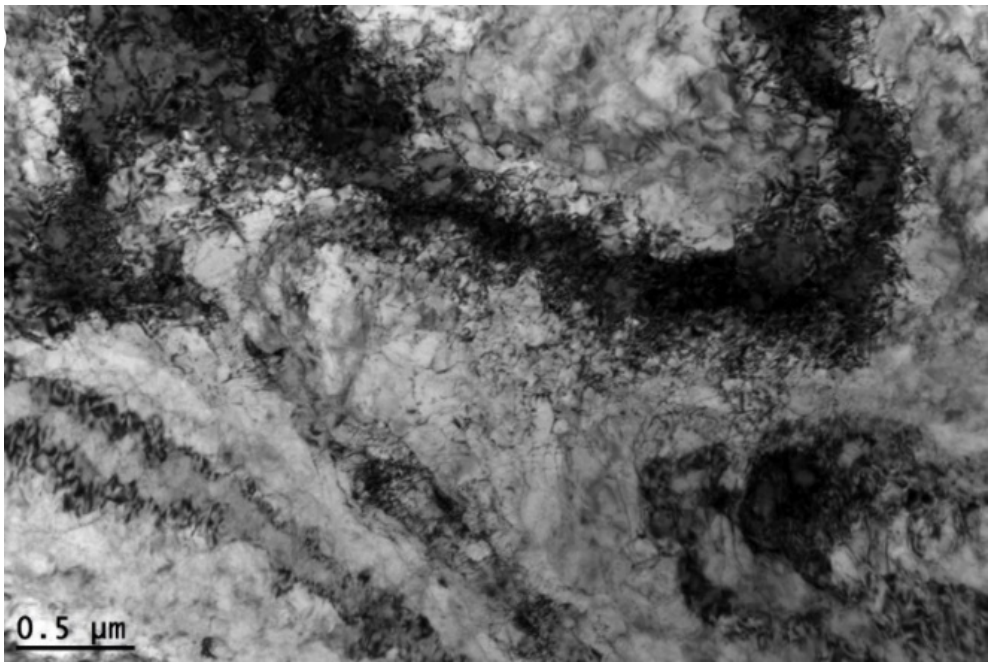

(b)

Fig. 8 TEM images of CT sample with (a) lower and (b) higher different magnifications

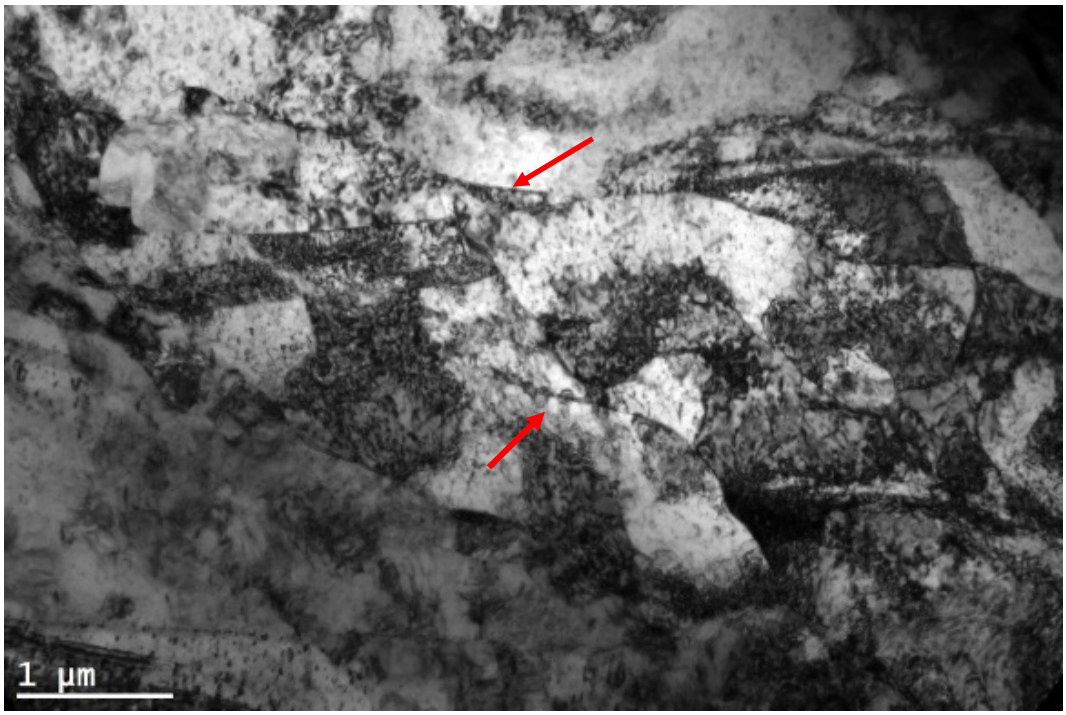

(a)

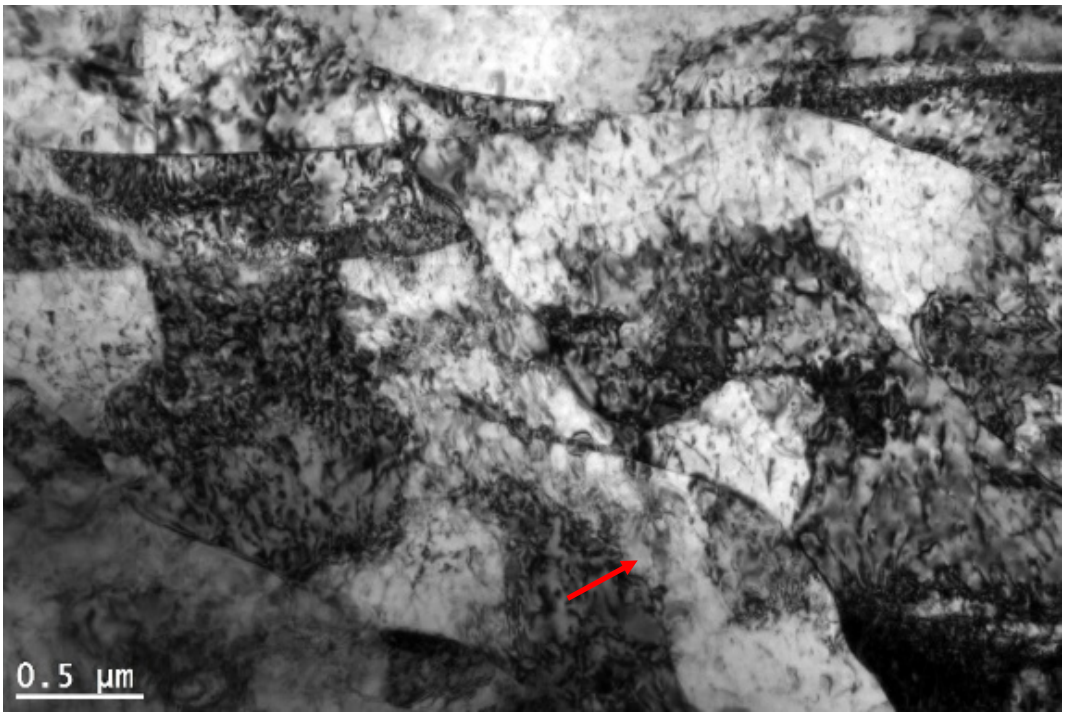

(b)

Fig. 9 TEM images of WCT sample with (a) lower and (b) higher different magnifications

Tables

Samples	1. Pass	2. Pass
Combined Temperature (CT)	450 ˚C	100 ˚C
Warm Temperature (WT)	450 ˚C	450 ˚C

Table 1. ECAP samples and their pressing temperatures

Samples	Yield MPa	Maximum Tensile Strength MPa	Young Modulus GPa	Hardness $H_{v0.2}$
Initial	553.22	612.78	161	179.84
CT	757.82	792.34	143	272.18
WT	712.11	758.40	152	244.59

Table 2. Mechanical test results of specimen